CHAPTER FOUR

Polymerization of Ethylene-SMRCV Using CI[1]

4.1 INTRODUCTION

4.1.1 Natural rubber

Five hundred years ago, on 11th of June 1496, Christopher Columbus brought back the first rubber balls from the West Indies. This marked the beginning of natural rubber (Baker, 2003). Natural rubber contains cis-1,4-polyisoprene that makes it a good elastic properties, resilience and damping behavior but poor chemical resistance and processing ability. Natural rubber also possesses a high molecular weight turning it into a highly stereoregular microstructure which produces unique mechanical properties. A high number of double bonds in the chemical structure makes it poor in resistance to heat, oxygen and ozone (Yahya, *et al.*, 2011).

Natural rubber generally was found tough in crude form but becomes soft and sticky when exposed to the high temperature. Natural rubber has 0.915 specific gravity. The most important property of natural rubber is the elasticity, stretchable when expanded and regained to original shape when released as the structure molecules was coiled like. Raw natural rubber is low in tensile strength and abrasion resistance and absorbs huge quantities of water, insoluble in water, acetone, alcohol, alkalis and dilute acids. However, pure natural rubber is amorphous solid, transparent and becomes crystalline with long period of cooling (Du *et al.*, 2010)

Modifications of natural rubber are made not only to enhance of certain properties characteristic but to introduce new properties associated with natural rubber. The modifications were carried out as natural rubber is a very important elastomeric material due to the excellent physical properties of natural rubber and the fact that it is a renewable resource (Lehrle & Willis, 1997).

4.1.2 Standard Malaysia Rubber Constant Viscosity (SMRCV)

SMR is a type of natural rubber which is being named in 1965 because it is a Malaysian-made rubber. The advantages of SMR products are higher uniformity, greatly improved cleanliness, and better appearance, as well as ease of handling from the producing workplace (Kwo, 2007). SMR was graded based on its cleanliness or maximum dirt content and the extent of some other foreign contaminants, such as copper, manganese, nitrogen, and volatile constituents. There are few types of SMR that are divided into different grades such as SMR 5, SMR 5L, SMR 10, SMR 20, SMR 50, SMR EQ, SMR GP, SMRCV and SMRLV.

SMRCV is one of Malaysian-made natural rubber produced from high quality latex, coagulated with control methods to produced low *lovibond* and stabilized Mooney Viscosity. SMRCV is widely used in daily activities as mechanical mountings for engines and machinery, general automotive components and injection moulded goods, including rubber-to-metal bonded components (Fan *et al.*, 2010). This is because the properties of SMRCV are a coherent bond, thus increasing milling throughput. The processability of SMRCV will not be affected during storage, as evidenced by the insignificant increase in the Mooney viscosity value with time. Moreover, SMRCV permits higher curing temperature due to constant viscosity features.

4.1.3   Grafting with natural rubber

The polymer properties can be improved by modification using several techniques such as blending, curing and grafting. Blending is a physical process where two or more polymers form the requisite properties. Curing is the polymerization of an oligomer mixture to produce a coating that adheres to the substrate through physical forces. Grafting is a process to introduce monomers to the polymer chain via covalent bond, where generally, the side-chains and the main chain is different in constitutional or configurational features (Bhattacharya & Misra, 2004).

Graft co-polymerization was carried out via several techniques such as chemical, radiation, photochemical, plasma-induced techniques and enzymatic grafting (Bhattacharya & Misra, 2004; Matyjaszewski, n. d.). Usually the backbone of the graft copolymer is made from thermoplastic materials such as polypropylene, polyethylene, polystyrene and polyester (Nakason, *et al.*, 2004). Dafader, *et al.* (2006) reported that by grafting with natural rubber, some properties such as tensile properties, wettability, and biocompatibility were improved. As an example, George, *et al.* (2003) reported grafting modification which involves a natural rubber with olefinic monomers like styrene acrylonitrile and methyl methacrylate (MMA) to form hard plastic materials.

4.2   EXPERIMENTAL

4.2.1. Preparation of SMRCV-toluene solution

SMRCV was obtained from Lembaga Getah Malaysia. A block of SMRCV was cut to small pieces before weighing and dissolved in toluene. The amounts of SMRCV used depend on the percentage of weight over volume (w/v %) of SMRCV-toluene solution. The SMRCV was stirred to dissolve in toluene solvent. Preparation of SMRCV-toluene solution was performed under nitrogen atmosphere. The solutions are stored in dry box before use.

4.2.2. Polymerization of Ethylene-SMRCV

Polymerization of ethylene-SMRCV was performed by applying procedures described in **Sections 3.2.3** and **3.2.4**. The catalyst system used in the polymerization was a combination of **CI[1]** with $AlEt_2Cl$ as cocatalyst. The Al/Cr molar ratio was standardized to 26.2 for all series of polymerizations. 0.02 g of **CI[1]** was placed in a reactor flask. The SMRCV-toluene solution prepared in **Section 4.2.1** was measured using syringes and transferred into the reactor flask followed by cocatalysts. After that, the reactor flask was attached to the gasline to start the polymerization process. The polymerization was performed at $30^{o}C$ and 1 atm atmosphere for 60 minutes. Eventually, the solution containing the polymer was poured into a solution of HCl-methanol and filtered before washing thoroughly with methanol. The polymer was dried under vacuum oven for 24 hours and the weight was recorded.

Table 4.1 presents the polymerization of ethylene-SMRCV system where the amounts of SMRCV in toluene solvent were varied from 0.0% to 1.0%. The polymerization was standardized by using **CI[1]** as catalyst, AlEt$_2$Cl as cocatalyst and the molar ratio was constant at 26.2. Furthermore, the polymerizations were performed at 30°C under 1 atm pressure.

Table 4.1: Variation of SMRCV added in the polymerization

Polymer	Amount of SMRCV in solvent (w/v %)
PE-SMRCV(0.0%)	0.0
PE-SMRCV(0.3%)	0.3
PE-SMRCV(0.5%)	0.5
PE-SMRCV(0.7%)	0.7
PE-SMRCV(1.0%)	1.0

* PE-SMRCV(0.0%) = PE-**CI[1]**

4.2.3. Characterization of polymer

The polymer products were characterized using IR spectroscopy, TGA and X-ray diffraction analysis.

a) *IR spectroscopy*

IR spectrum was recorded using ATR-IR spectrometer model Perkin Elmer spectrum 400 FT-IR/FT-FIR from Perkin Elmer, US. The IR spectrum was analysed in range of 4000 – 600 cm^{-1}.

b) *Thermal gravimetric analysis (TGA)*

TGA analysis was carried out using TGA analyser model Pyris Diamond TG/DTA from Perkin Elmer, US. The polymer sample analysed in temperature range of $50 - 900^{\circ}C$ with scan rate of $20^{\circ}C$/min. The analysis was performed under nitrogen atmosphere and nitrogen flow rate was set to 20 ml/min.

c) *Powder X-ray Diffraction (XRD) analysis*

XRD analysis was performed using an X-Ray Diffractometer (PANalytical X'Pert Pro Multipurpose diffractometer, PANalytical Co. Netherlands). The X-ray diffraction patterns were recorded in reflection mode at 40 kV, 40 mA from 5° 2θ to 80° 2θ with step size of 0.02° 2θ. Source used were Cu ($K\alpha1$ wavelength 1.54060 Å) and the divergence slit size was 0.1089°.

4.3   RESULTS AND DISCUSSION

4.3.1. Polymerization of ethylene-SMRCV

The polymerization of ethylene-SMRCV process was performed for 60 minutes at $30^{\circ}C$ under 1 atm pressure. As soon as the cocatalyst was introduced into reactor flask, the solution changed from a clear solution to yellowish-green solution. This indicates that reaction between catalyst and cocatalyst had occurred where Cr^{3+} was reduced to Cr^{2+} (Gan, *et. al*, 1987; Soga, *et al.*, 1985a, 1985b). When the ethylene monomer started to polymerize, the yellowish-green solution turned to yellow and at the end of the process, the solution turned to cloudy-orange.

Higher rate of polymerization is found in the first 20 minutes as shown in **Figure 4.1**. Pressure dropped drastically in this period, indicating more of the monomer gas was used within this time. This period is the critical period for polymerization as the activity of polymerization is the highest within this period. After that, pressure dropped and the rate of polymerization declined steadily until the end of polymerization. The polymer started to form as soon as the ethylene monomer was introduced to the reactor flask. At the end of the process, a white mucous-like polymer solution was produced. The solution was poured into a mixture of methanol-HCl. After filteration, the polymer was washed thoroughly with methanol then dried at 60°C for 24 hours.
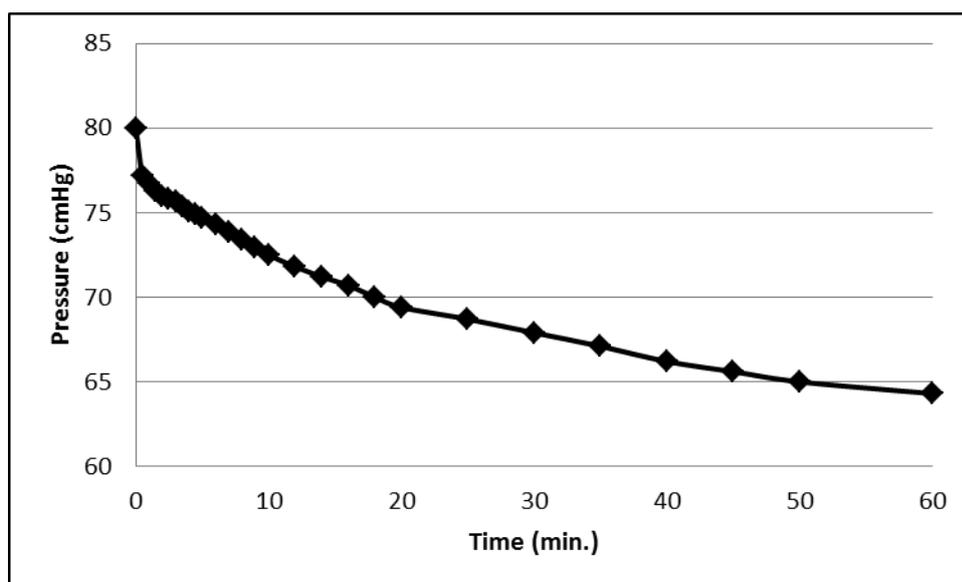
Figure 4.1: Plot of pressure versus time for the polymerization of ethylene-SMRCV(1.0%)
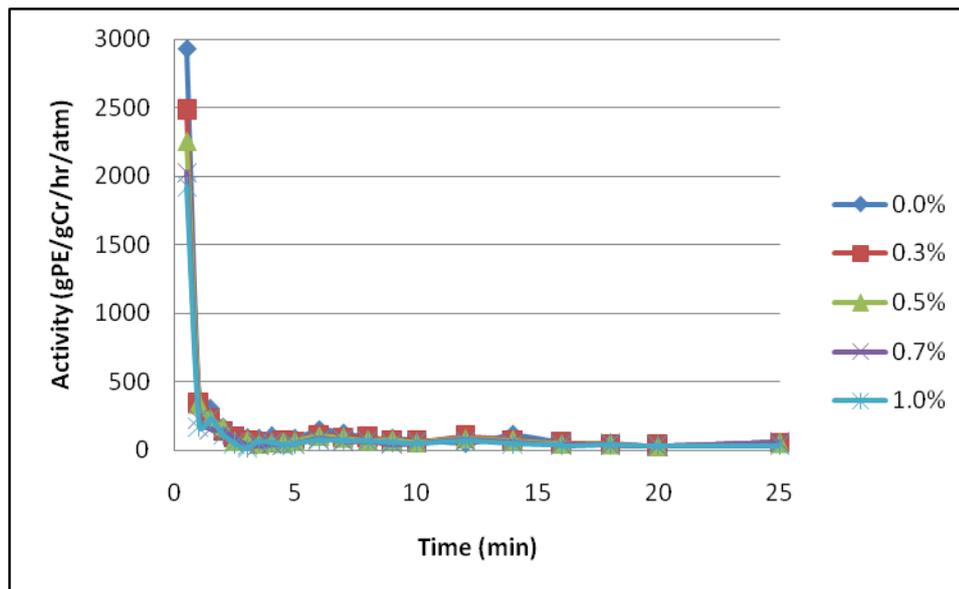
Figure 4.2: Kinetic curve for the polymerization of ethylene-SMRCV

Most of the catalyst-olefin systems are the decaying type in which the rate curve reaches a maximum and then continues to decline. The rate of decline varies according to the catalyst-monomer system. Increasing in the time of polymerization, the decline in rate becomes smaller (Boor, 1979; Keii, 1972).

Kinetic curves for the series of polymerization of ethylene-SMRCV are plotted in **Figure 4.2**. The curves show that the catalytic activity for the polymerization is a decaying type, as agreed by Boor (1979) and Keii (1972). As soon as the polymerization started, the catalytic acitivity rose to the highest level. Then it decreased steadily to the end of polymerization.

Highest catalytic activity was found in the critical period where PE was produced the most. The highest activity occurred at early period of polymerization process. This is due to the breaking of the catalyst particle and the exposure of new surfaces and the formation new active centres for polymerization process. However, the activity decreased gradually with time attributed to the active centres becoming unstable due to some structural changes (Gan, *et al.*, 1987).

The rate of PE formation decreased after 20 minutes as the active sites were reduced in the polymerization process and the accretion of solution viscosity. Furthermore, the formation of PE decreased because the monomer gas could not reach the active sites due to encapsulation of active site by newly formed PE. The PE which was formed aggressively in the early period of polymerization results in accumulation of PE. In addition, the precipitation of PE has led to non-uniform stirring hence decreasing the rate of polymerization (Gan, *et al.*, 2000). Keii *et al.* (1972) found that the rate of polymerization was proportional to the stirring speed due to the mass transfer effect.

Polymerization mechanism has been proposed in three steps which is initiation, propagation and chain termination steps (Boor, 1979). The propagation steps plays an important role in kinetic of the polymerization process (Huang & Rempel, 1995). **Figure 4.3** shows plot of ℓn P versus time for the polymerization of ethylene-SMRCV(1.0%) using **CI[1]** and Al/Cr ratio of 26.2 at 30°C. The plot demonstrates a straight line in the first 10 minutes indicating the reaction was a first order reaction. The linearity then started to deviate due to the deactivation of active centres.
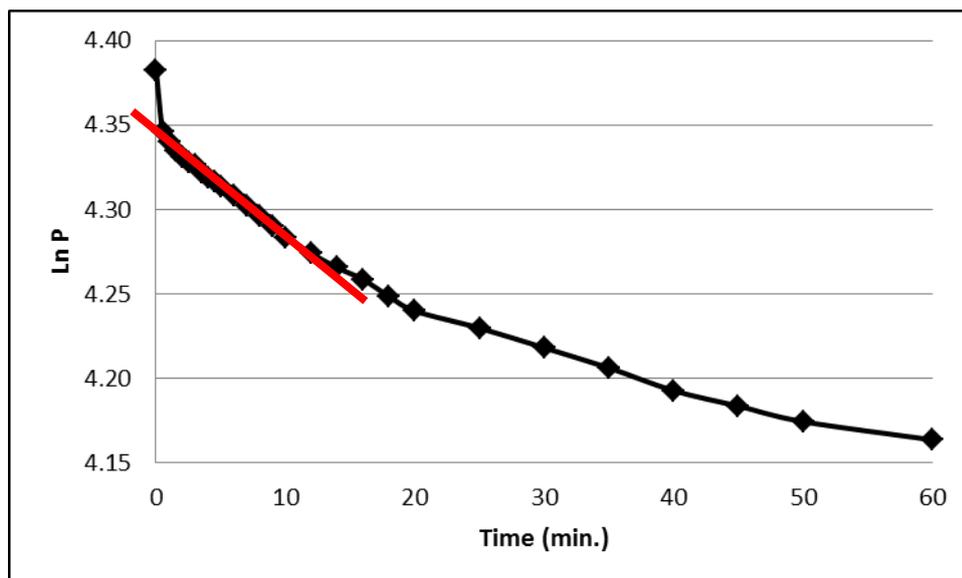
Figure 4.3: Plot ℓn P versus time for the polymerization of ethylene-SMRCV(1.0%)

4.3.2. Effect of addition of SMRCV

The polymerization of ethylene-SMRCV was carried out by dissolving an amount of SMRCV in toluene solution. The effect of rubber in polymerization of ethylene is still unknown and yet to be discovered. The SMRCV was suspected to graft with PE or act as a support for the polymerization of ethylene. Some researchers have used natural rubber to be grafted with polystyrene (Suksawad, *et al.*, 2011), methyl methacrylate (Lehrle & Willis, 1997) and other polymer (Derouet, *et al.*, 2009; Oliveira *et al.*, 2005)
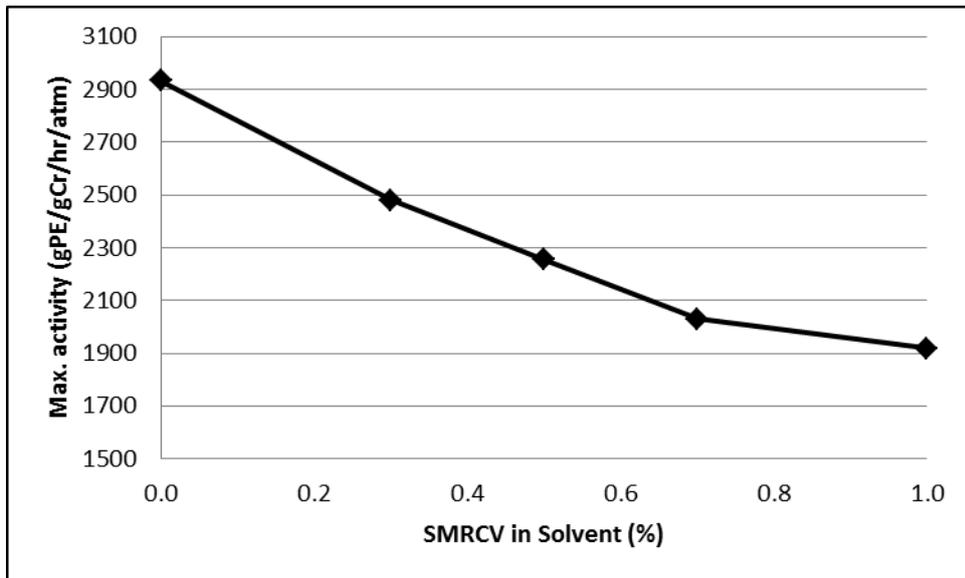
Figure 4.4: Plot of maximum initial activity versus percentage of SMRCV in toluene

for the polymerization of ethylene-SMRVC
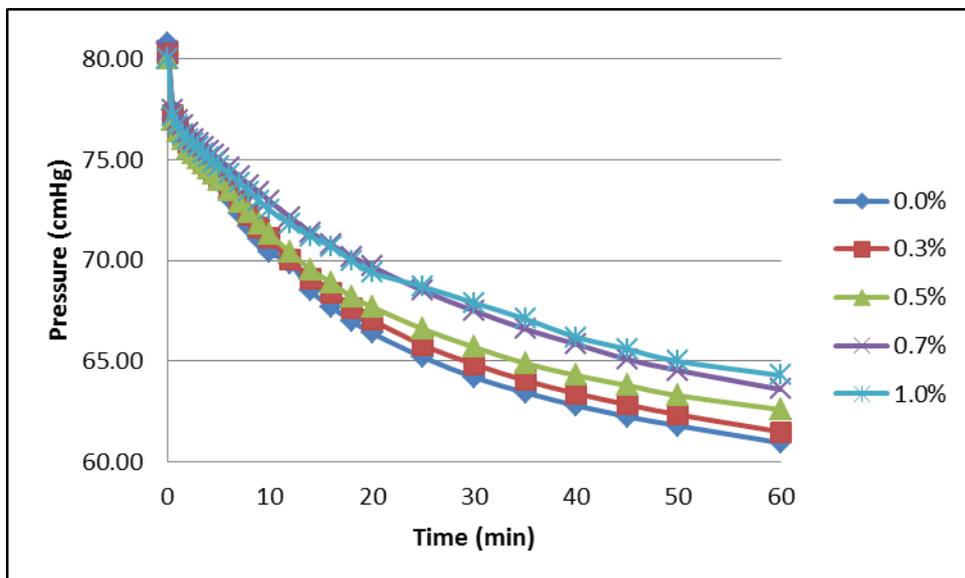
Figure 4.5: Plot pressure drop versus time for the polymerization of ethylene-SMRCV

Series of polymerizations were carried out to study the effect of the addition of SMRCV towards polymerization of ethylene by varying the amounts of SMRCV in solution. **Figure 4.4** shows the addition of SMRCV influences the maximum initial activity of polymerization. The maximum initial activity is found to decrease as the amount of SMRCV in solution is increased. This proves that the presence of SMRCV causes the rate of polymerization to decrease.

Figure 4.5 shows the pressure drop versus time that represents the amount of monomer used. The usage of monomer gas in the polymerization process was found to decline with higher amount of SMRCV added into the toluene. This shows that the rate of PE formation also decreased. The addition of SMRCV leads to the accretion of solution viscosity. Therefore, it is harder for the monomer to react with the catalysts systems, as the active sites were encapsulated by the SMRCV.

Table 4.2: Catalytic activity and total pressure drop for the polymerization of ethylene-SMRCV

Amount of SMRCV (%)	Max. initial Activity (gPE/gCr/hr/atm)	Total pressure drop (cmHg)
0.0	2932	39.7
0.3	2481	37.6
0.5	2255	34.8
0.7	2030	33.6
1.0	1917	31.4

Table 4.2 presents the maximum initial activity and the total pressure drop of monomer gas for the polymerization of ethylene-SMRCV. The maximum initial activity decreased from 2932 gPE/gCr/hr/atm to 1917 gPE/gCr/hr/atm as 1.0% of SMRCV was added to the polymerization system. Meanwhile, the rate of monomer gas usage also decreased by 8.3 cmHg (39.7 − 31.4 cmHg). It is believed that the addition of SMRCV has interfered with the polymerization. The involvement of SMRCV into the polymerization of ethylene is described in **Section 4.3.3**.

4.3.3. Characterization of polymer

a) *IR spectroscopy*

IR spectra analysis was carried out to determine the occurrence of SMRCV in PE. IR spectrum for raw SMRCV is compared with the PE-SMRCV shown as in **Figure 4.6**. The IR spectrum of SMRCV exhibits the natural rubber absorption bands with bands appearing at 841 cm^{-1} (C=CH deformation), 1444 cm^{-1} (CH_3 and CH_2 deformations), and 1376 cm^{-1} (CH_3 deformation) (Cook, *et al.*, 1997; Nakason, *et al.*, 2004).
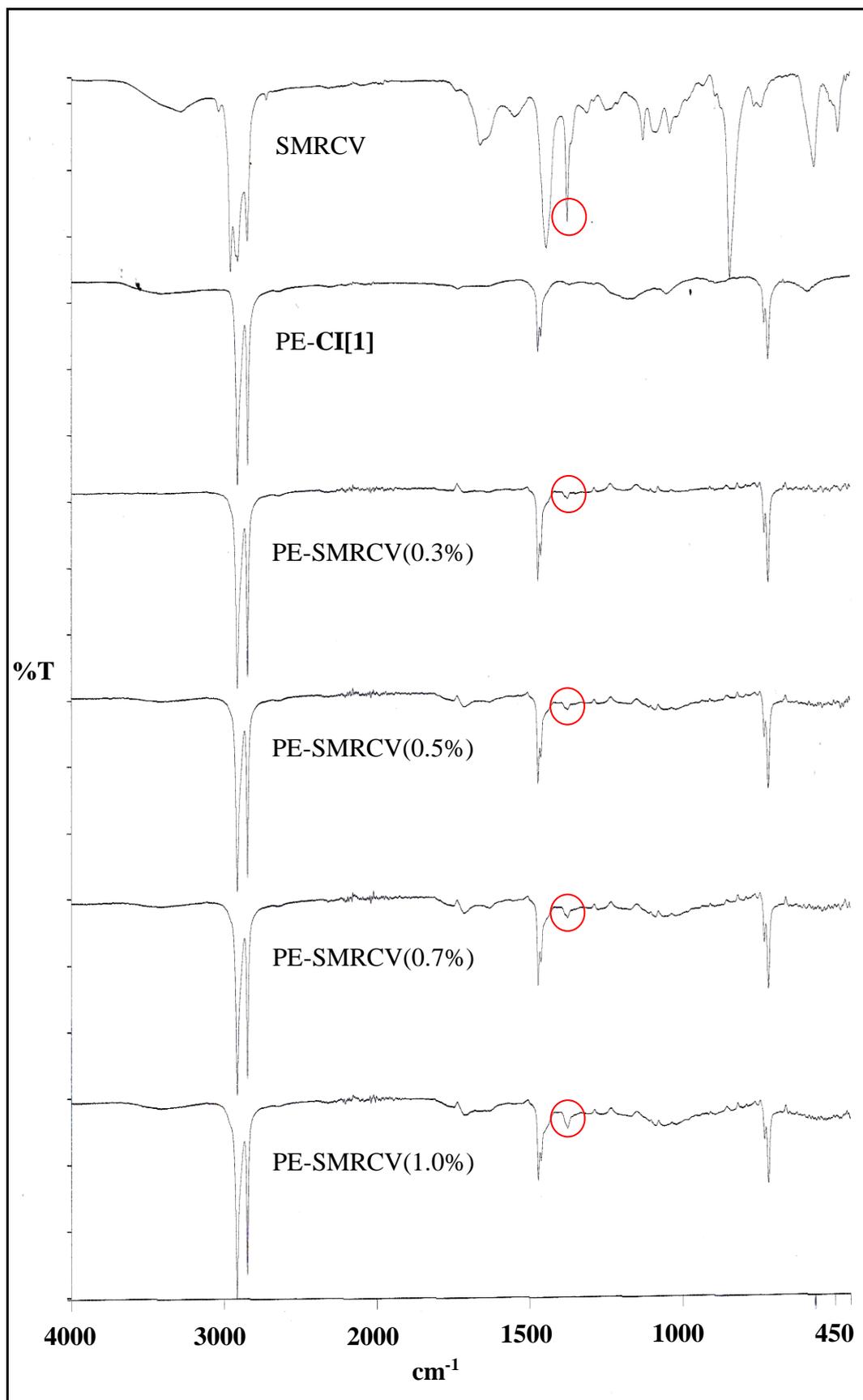
Figure 4.6: IR spectra for SMRCV (natural rubber), PE-**CI[1]**, PE-SMRCV(0.3%), PE-SMRCV(0.5%), PE-SMRCV(0.7%) and PE-SMRCV(1.0%)

Table 4.3 presents the assignment of IR spectra for PE-**CI[1]**, PE-SMRCV(0.3%), PE-SMRCV(0.5%), PE-SMRCV(0.7%) and PE-SMRCV(1.0%). The characteristic bands of PE are present in all spectra where the bands appear at $\nu_{asym}(CH_2)$ 2915 cm^{-1}, $\nu_{sym}(CH_2)$ 2848 cm^{-1}, $\delta(CH_2)$ 1472 cm^{-1}, 1463 cm^{-1}, $\nu_{rocking}(CH_2)$ 730 cm^{-1} and 717 cm^{-1} (Hagemann, *et al.*, 1989; Jones & Lauer, 1979; Rojas, *et al.*, 1997; Krimm, 1956). However, $\delta_{sym}(CH_3)$ which is absent in PE-**CI[1]** spectrum is found to appear in all PE-SMRCV spectra. A medium band assigned to CH_3 deformation is observed at 1376 cm^{-1} indicating that the SMRCV is attached to the PE. Some of SMRCV's bands are found to be absent in PE-SMRCV's bands possibly due to overlapping with PE's bands. One of the SMRCV's bands that is found to disappear was C=CH deformation bands at 841 cm^{-1}.

Table 4.3: Band assignment for IR spectrum of PE-SMRCV

Band assignment	Group frequency, wavenumber (cm^{-1})				
	PE-SMRCV (0.0%)	PE-SMRCV (0.3%)	PE-SMRCV (0.5%)	PE-SMRCV (0.7%)	PE-SMRCV (1.0%)
$\nu_{asym}(CH_2)$	2915	2915	2915	2915	2915
$\nu_{sym}(CH_2)$	2848	2848	2848	2848	2848
$\delta(CH_2)$	1472, 1463	1472,1463	1472,1463	1472,1463	1472,1463
$\delta_{sym}(CH_3)$	-	1376	1376	1376	1376
$\nu_{rocking}(CH_2)$	730, 717	730, 717	730, 717	730, 717	730, 717

b) *Thermal gravimetric analysis (TGA)*

TGA curves were recorded from 50 to 900ºC at 20ºC/min to study the thermal stability of polymer. **Figure 4.7** displays the plots of percentage of weight loss versus temperature for SMRCV, PE-**CI[1]**, PE-SMRCV(0.3%), PE-SMRCV(0.5%), PE-SMRCV(0.7%) and PE-SMRCV(1.0%). **Table 4.4** also presents the information of the thermograms.
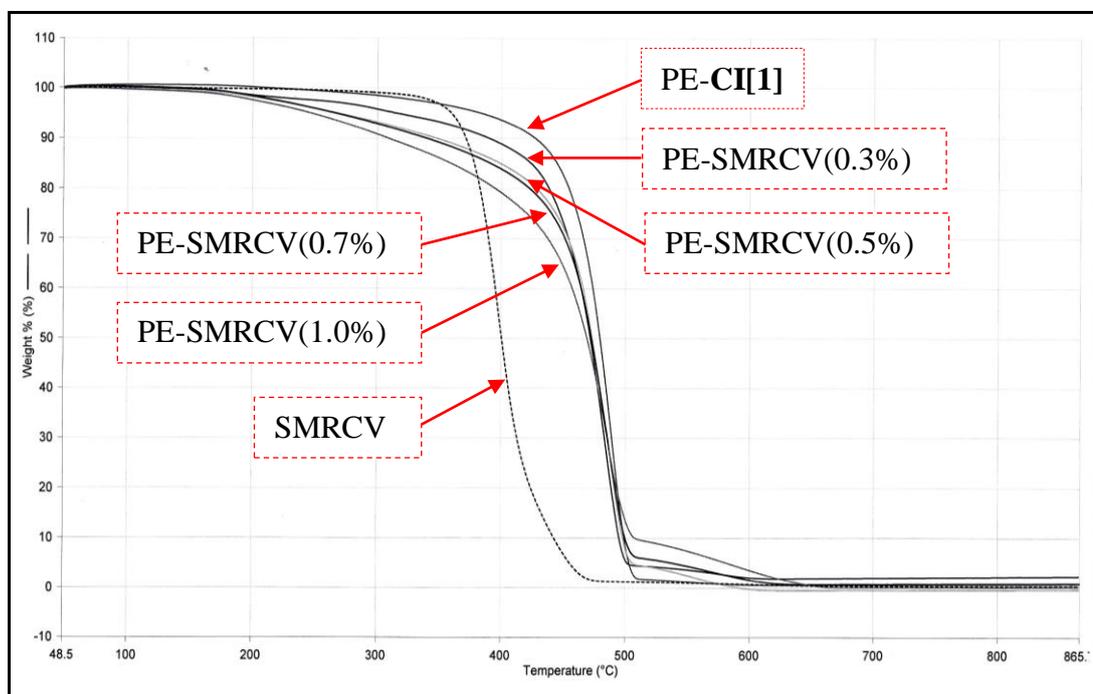
Figure 4.7: Thermogram of SMRCV, PE-**CI[1]**, PE-SMRCV(0.3%), PE-SMRCV(0.5%), PE-SMRCV(0.7%) and PE-SMRCV(1.0%)

Table 4.4: The percentage of weight loss, range of degradation, onset temperature

(T_{onset}) and derivative peak temperature (DT_p) of polymer

Polymer	Weight loss (%)		Range of degradation (^{o}C)	T_{onset} (^{o}C)	DT_p (^{o}C)
	1st step	2nd step			
SMRCV	99.7	-	262 – 487	372	399
PE-SMRCV(0.0%)	99.5	-	180 – 593	455	487
PE-SMRCV(0.3%)	95.2	2.6	178 – 621	447	484
PE-SMRCV(0.5%)	94.8	5.0	178 – 622	441	484
PE-SMRCV(0.7%)	93.8	5.3	178 – 643	438	482
PE-SMRCV(1.0%)	89.7	9.4	178 – 668	425	482

* PE-SMRCV(0.0%) = PE-**CI[1]**

The SMRCV thermal curve recorded as a reference showed an obvious difference with the PE thermal curve where the degradation temperature started at 262°C and ended at 487°C. The SMRCV degraded in a single step with T_{onset} at 372°C and DT_p at 399°C (Derouet, *et al.*, 2009). SMRCV was completely degraded with residue of just about 0.3%.

The degradation of PE-**CI[1]** was decomposed in a single step (Section 3.3.7b) while the degradation of SMRCV grafted PE was found to decompose in two steps. The range of decomposition for PE-SMRCV (**Table 4.4**) is dependent on the percentage of SMRCV present. The temperature where the PE-SMRCV completely degrade increased with increasing SMRCV content. However, the initial degradation temperature and DT_P for PE-**CI[1]**, PE-SMRCV(0.3%), PE-SMRCV(0.5%), PE-SMRCV(0.7%) and PE-SMRCV(1.0%) showed insignificant change. The initial degradation temperature was in 178 – 180°C region and the DT_p was in 482 – 487°C region. Moreover, the second step degradation for all PE grafted SMRCV started at 510°C.

The degradation of PE grafted with SMRCV happens in two steps where the percentage of weight loss for the first and second degradation is summarized in **Table 4.4**. The weight loss for the first step degradation is found to decreases while the second step increases with amount of SMRCV added. It is believed that the addition of SMRCV leads to the formation of new stable branches that degrade in the second step. Nevertheless, the structure is yet to be discovered.

The TGA curves (**Figure 4.7**) demonstrate that the addition of SMRCV in PE deteriorates the thermal stability of PE-SMRCV. The T_{onset} for PE-SMRCV decreases from 455°C to 425°C as the SMRCV is added as shown in **Table 4.4**. However, the T_{onset} of PE-SMRCV is much higher than the T_{onset} of SMRCV which is only 372°C. Based on T_{onset}, the initial thermal stability of PE-SMRCV is found to decrease as the SMRCV is added to the polymerization system but higher than the pure SMRCV (Rahman, *et al.*, 2012).

c) *Powder X-ray Diffraction (XRD) analysis*

XRD for the polymers were recorded from $2\theta = 5°$ to $2\theta = 80°$ (**Figure 4.8**). XRD patterns for orthorhombic PE appear as two crystalline peaks, the more intense with Miller index of (110) and the less intense with Miller index of (200), overlapped to the amorphous *halo*. The (110) and the (200) peaks are observed at 21.3° and at 24.0° (Sami, *et al.*, 2010; Baker & Windle, 2001; Moysés & Machado, 2002). Broad peaks referred to the rubber's characteristic peaks are observed at 14° (Johns & Rao, 2009; Tantatherdtam & Sriroth, n. d.). The XRD patterns of PE-SMRCV(0.3%), PE-SMRCV(0.5%), PE-SMRCV(0.7%) and PE-SMRCV(1.0%) showed the bands, but the band was found to be absent for PE-**CI[1]** XRD pattern.
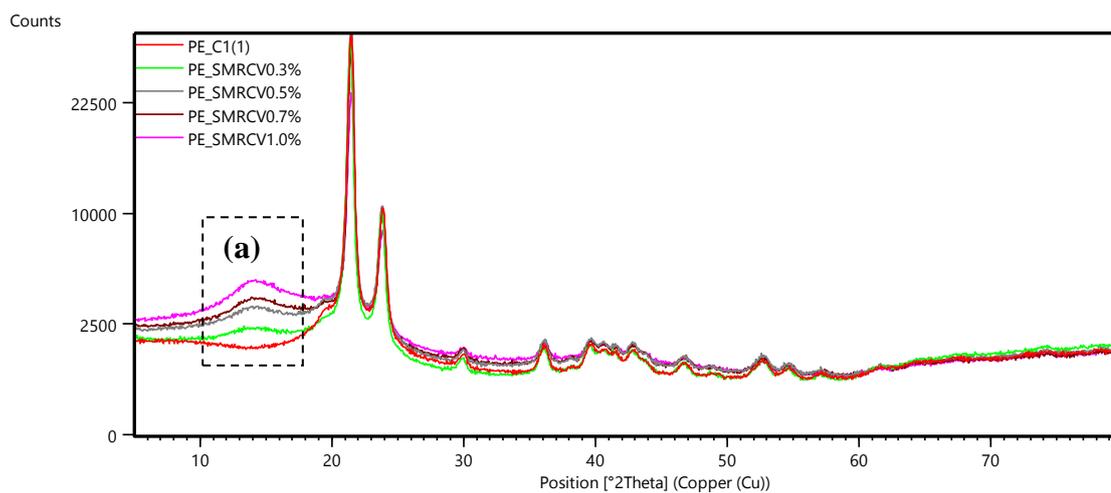
Figure 4.8: XRD of PE-**CI[1]**, PE-SMRCV(0.3%), PE-SMRCV(0.5%), PE-

SMRCV(0.7%) and PE-SMRCV(1.0%)

Table 4.5: Intensity of peak at $2\theta = 14^\circ$ and percentage of crystallinity

Polymer	Intensity of peak $2\theta = 14^\circ$ (Counts)	Percentage of Crystallinity (%)
PE-CI[1]	1593	47.8
PE-SMRCV(0.3%)	2346	45.4
PE-SMRCV(0.5%)	3347	40.7
PE-SMRCV(0.7%)	3858	40.4
PE-SMRCV(1.0%)	4863	33.6

The XRD patterns were analysed using HighScore Plus software, where the percentage of crystallinity and the intensity (Counts unit) of bands were determined. **Table 4.5** shows the intensity of peak $2\theta = 14^{o}$ (amorphous halo) and the percentage of crystallinity for polymers. The intensity of rubber peak is found to increase from 1593 – 1863 counts as the amount of SMRCV added is increased from 0.0 – 1.0% (box **(a)** in **Figure 4.8**). Meanwhile, the percentage of crystallinity decreased as higher amount of SMRCV was added in polymerization system. The addition of SMRCV towards PE leads to increase the amorphous properties of polymer.

References

A. Sami, David, E., & Fréchette, M. (2010). Procedure for evaluating the crystallinity from X-ray diffraction scans of High and Low Density Polyethylene/SiO$_2$ Composites. *2010 Annual Report Conference on Electrical Insulation and Dielectric Phenomena.* Retrieved from http://ieeexplore.ieee.org/stamp/stamp.jsp?arnumber=05724069

Baker, A. M. E., & Windle, A. H. (2001). Evidence for a partially ordered component in polyethylene from wide-angle X-ray diffraction. *Polymer, 42*(2), 667-680.

Bhattacharya, A., & Misra, B. N. (2004). Grafting: a versatile means to modify polymers: Techniques, factors and applications. *Progress in Polymer Science, 29*(8), 767-814.

Boor, J. (1979). *Ziegler-Natta catalysts and polymerizations.* New York: Academic Press.

Cook, J. W., Edge, S., & Packham, D. E. (1997). Infrared spectroscopic studies of the interaction between natural rubber and chlorinated natural rubber. *Journal of Materials Science Letters, 16*(6), 445-447.

Dafader, N. C., Haque, M. E., Akhtar, F., & Ahmad, M. U. (2006). Study on grafting of different types of acrylic monomers onto natural rubber by γ-rays. *Radiation Physics and Chemistry, 75*(1), 168-172.

Derouet, D., Intharapat, P., Tran, Q. N., Gohier, F., & Nakason, C. (2009). Graft copolymers of natural rubber and poly(dimethyl(acryloyloxymethyl)phosphonate) (NR-g-PDMAMP) or poly(dimethyl(methacryloyloxyethyl)phosphonate) (NR-g-PDMMEP) from photopolymerization in latex medium. *European Polymer Journal, 45*(3), 820-836.

Du, L., Li, W., Fan, L., Jiang, B., Wang, J., Yang, Y., *et al.* (2010). Hybrid titanium catalyst supported on core-shell silica/poly(styrene-co- acrylic acid) carrier. *Journal of Applied Polymer Science, 118*(3), 1743-1751.

Fan, L., Du, L., Huang, H., Zhang, L., Jiang, B., Wang, J., *et al.* (2010). Ethylene polymerization with core-shell ziegler-natta hybrid catalysts. *Acta Polymerica Sinica*(8), 981-986.

Gan, S. N., Aishah, M. J., & Ooi, C. P. (2000). Trinuclear oxo-centered chromium(III) carboxylate complexes as Ziegler-Natta catalysts for ethylene polymerization. In T. Sano, Uozumi, T., Nakatani, H and Terano, M. (Ed.), *Progress and Development of Catalytic Olefin Polymerization* (pp. 25-32). Tokyo: Technology and Education Publishers.

Gan, S. N., Chen, S. I., Ohnishi, R., & Soga, K. (1987). Homo- and copolymerization of ethylene and propylene using a heterogeneous chromium catalyst system. *Polymer, 28*, 1391-1395.

George, V., Britto, I. J., & Sebastian, M. S. (2003). Studies on radiation grafting of methyl methacrylate onto natural rubber for improving modulus of latex film. *Radiation Physics and Chemistry, 66*(5), 367-372.

Hagemann, H., Snyder, R. G., Peacock, A. J., & Mandelkern, L. (1989). Quantitative infrared methods for the measurement of crystallinity and its temperature dependence: polyethylene. *Macromolecules, 22*(9), 3600-3606.

Huang, J., & Rempel, G. L. (1995). Ziegler-Natta catalysts for olefin polymerization: Mechanistic insights from metallocene systems. *Progress in Polymer Science, 20*(3), 459-526.

Johns, J., & Rao, V. (2009). Thermal stability, morphology, and X-ray diffraction studies of dynamically vulcanized natural rubber/chitosan blends. *Journal of Materials Science, 44*(15), 4087-4094.

Jones, W. R., & Lauer, J. L. (1979). INFRARED ANALYS IS OF POLYETHYLENE WEAR SPECIMENS US ING ATTENUATED TOTAL REFLECTION SPECTROSCOPY. *NASA Technical Memorandum 79228*. Retrieved from http://ntrs.nasa.gov/archive/nasa/casi.ntrs.nasa.gov/19790021158_1979021158.pdf

Keii, T. (1972). *Kinetics of Ziegler-Natta polymerization*. Tokyo: Kodansha.

Krimm, S. C. Y. L., and G. B. B. M. Sutherland. (1956). Infrared Spectra of High Polymers. II. Polyethylene. *The Journal Of Chemical Physics, 25*(3), 549 - 562.

Kwo, H. K. (2007). *STUDY OF ADHESION PROPERTIES OF NATURAL RUBBER, EPOXIDIZED NATURAL RUBBER, AND ETHYLENE-PROPYLENE DIENE TERPOLYMER-BASED ADHESIVES*. Master of Science, Universiti Sains Malaysia, Pulau Pinang.

Lehrle, R. S., & Willis, S. L. (1997). Modification of natural rubber: A study to assess the effect of vinyl acetate on the efficiency of grafting methyl methacrylate on rubber in latex form, in the presence of azo-bis-isobutyronitrile. *Polymer, 38*(24), 5937-5946.

Matyjaszewski, K. (n. d.). Graft Copolymers. *Preparation of Functional Materials*. Retrieved from http://www.cmu.edu/maty/materials/Synthesis_of_well_defined_macromolecules/graft-copolymers.html

Moysés, S. C., & Machado, R. (2002). A study of melting of low density polyethylene by in situ WAXD. *European Polymer Journal, 38*(10), 2041-2044.

Nakason, C., Kaesaman, A., & Supasanthitikul, P. (2004). The grafting of maleic anhydride onto natural rubber. *Polymer Testing, 23*(1), 35-41.

Oliveira, P. C., Guimarães, A., Cavaillé, J.-Y., Chazeau, L., Gilbert, R. G., & Santos, A. M. (2005). Poly(dimethylaminoethyl methacrylate) grafted natural rubber from seeded emulsion polymerization. *Polymer, 46*(4), 1105-1111.

Rahman, N. A., Hassan, A., Yahya, R., Lafia-Araga, R. A., & Hornsby, P. R. (2012). Micro-structural, thermal, and mechanical properties of injection-molded glass fiber/nanoclay/polypropylene composites. *Journal of Reinforced Plastics and Composites, 31*(4), 269-281.

Rojas, B. G., Fatou, J., Martinez, C., & Laguna, O. (1997). The characterization of high-density polyethylenes functionalized with diethylmaleate: Correlation between FT-IR and 13C NMR data. *European Polymer Journal, 33*(5), 725-728.

Soga, K., Chen, S. I., Shiono, T., & Doi, Y. (1985a). Homo- and copolymerization of ethylene and propylene with a soluble chromium catalyst. *Polymer, 26*, 1888-1890.

Soga, K., Chen, S. I., Shiono, T., & Doi, Y. (1985b). Preparation of highly active Cr-catalysts for ethylene polymerization. *Polymer, 26*, 1891-1894.

Suksawad, P., Yamamoto, Y., & Kawahara, S. (2011). Preparation of thermoplastic elastomer from natural rubber grafted with polystyrene. *European Polymer Journal, 47*(3), 330-337.

Tantatherdtam, R., & Sriroth, K. (n. d.). Morphologies of Natural Rubber/Gelatinized Starch and Mineral Clay Composite. Retrieved from http://kucon.lib.ku.ac.th/Fulltext/KC4506023.pdf

Yahya, Y. S. R., Azura, A. R., & Ahmad, Z. (2011). Effect of Curing Systems on Thermal Degradation Behaviour of Natural Rubber (SMR CV 60). *Journal of Physical Science, 22*(2), 1–14.